JOURNAL OF CHEMICAL INFORMATION AND MODELING

Article

pubs.acs.org/jcim

Building a Three-Dimensional Model of CYP2C9 Inhibition Using the Autocorrelator: An Autonomous Model Generator

Matthew A. Lardy,*[,†] Laurie LeBrun,[‡] Drew Bullard, Charles Kissinger,[§] and Alberto Gobbi[⊥]

Anadys Pharmaceuticals, Inc., San Diego, CA, United States

ABSTRACT: In modern day drug discovery campaigns, computational chemists have to be concerned not only about improving the potency of molecules but also reducing any off-target ADMET activity. There are a plethora of antitargets that computational chemists may have to consider. Fortunately many antitargets have crystal structures deposited in the PDB. These structures are immediately useful to our Autocorrelator: an automated model generator that optimizes variables for building computational models. This paper describes the use of the Autocorrelator to construct high quality docking models for cytochrome P450 2C9 (CYP2C9) from two publicly available crystal structures. Both models result in strong correlation coefficients ($R^2 > 0.66$) between the predicted and experimental determined log(IC_{50}) values. Results from the two models overlap well with each other, converging on the same scoring function, deprotonated charge state, and predicted the binding orientation for our collection of molecules.

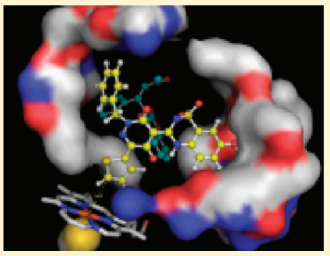

1. INTRODUCTION

Computational chemistry, when applied to drug discovery, has as its primary goal a deeper understanding of the interactions between proteins and ligands. In modern day discovery campaigns, this role has been expanded to include making predictions of ADMET properties of molecules and to provide interfaces to allow noncomputational chemists access to these predictions. These interfaces hold the promise of reducing the barrier of access for noncomputational chemists. This quiet transformation of computational chemistry has been most visible in occasional publications showcasing web-based interfaces.[1,2] These web-based platforms allow scientists direct access to computational models that have been created and optimized by computational chemists, eliminating a barrier between medicinal and computational chemists and allowing molecular designers to get predictions quickly.[3]

These platforms are ideal resources for noncomputational chemists to predict ADMET off-target activity like cytochrome P450 inhibition. Cytochrome P450s comprise a superfamily of heme-containing enzymes that oxidatively transform organic molecules.[4] These proteins, often referred to as CYPs, play an important role in the metabolism of many drugs. In fact, just five variants of cytochrome P450 (CYP2C9, CYP1A2, CYP2C19, CYP2D6, and CYP3A4) collectively metabolize 90% of drugs.[5] Of the variants of cytochrome P450 oxidases, CYP2C9 is one of the most prevalent. It constitutes approximately 20% of total hepatic P450 concentration. CYP2C9 is known to bind weak acids and is included as a standard enzyme screen by many pharmaceutical companies.

The metabolism of naturally occurring and synthetic organic molecules can be greatly reduced if CYPs are inhibited. This can lead to drug−drug interactions where the inhibition of a CYP by one drug increases the half-life of another drug, possibly increasing its toxicity. Drug−drug interactions are known to be problematic and require additional drug−drug interaction (DDI) studies.[6] Minimizing inhibition of CYPs is therefore an important part of the lead optimization process.

Several groups have published computational models predicting CYP2C9 inhibition. These models have varied in computational complexity from QSAR[7] to structural based docking approaches.[8] While QSAR models have shown a good correlation between experimental and computationally predicted IC_{50} values, they do not provide structural context explaining the CYP inhibition.[9] Docking models have taken advantage of two cocrystal structures deposited into the PDB (PDB codes: 1OG5 and 1R9O).[10,11] Docking against these structures provides hypothetical binding modes and have been used to produce models that are fairly accurate in the correlation of computational and experimentally determined potency.[12]

While docking approaches to the construction of models for CYP2C9 inhibition have been successful, recent work has taken a deeper look into the docking strategies themselves. Docking programs use novel strategies to predict the binding conformation of small molecules to a protein and to score those conformations according to their predicted binding energy. These strategies and empirically derived scoring functions are parametrized to yield good results by calibrating the parameters on a training set of known protein ligand complexes. Parameter values can vary greatly for specific applications. Recent work by Andersson et al. evaluated which parameters most greatly affect the ability of docking programs to reproduce the binding mode of published small molecule crystal structures.[13] In their work, they evaluated the effect of changing these docking parameters in two docking applications: GOLD[14] and FRED.[15] With GOLD they adjusted the parameters that configure the genetic algorithm, as well as the van der Waals and hydrogen bonding parameters. In FRED,

Received: November 23, 2011
Published: April 17, 2012

they changed the translational stepsize (tstep), the rotational stepsize (rstep), the scoring function, the negative image size (a parameter that controls how far away ligand atoms may be from the protein), and the van der Waals clash checking (clash). They tried a few variations of these parameters and docked ligands into a total of 68 complexes. The rmsd between the crystallographic and the docked pose was computed. Partial least squares (PLS) was used to determine which parameters had the greatest effect on good (rmsd <2 Å) docking results. With FRED they found that the selection of the scoring function had the greatest impact. In GOLD, the adjustment of the genetic algorithm parameters had the largest impact.

A docking model can be affected by many parameters. To explore all possible values a huge combinatorial space would have to be evaluated. The space becomes even larger when parameters of programs used to prepare the input molecules are considered. To address this problem, we have developed the Autocorrelator open source software that can automatically and autonomously evaluate the effect of varying the parameters on the docking model with the aim of finding optimal values for a specific docking application.[16] In addition, it can also optimize the scoring function by finding a new linear combination of scoring function components to fit the experimental data. The Autocorrelator has several approaches to evaluate the large parameter space, returning models with a high correlation between the resulting scoring function and experimental activities.

This paper describes the methodology used in the Autocorrelator application and then discusses the building of a docking model for prediction of the inhibition of CYP2C9 by molecules from Anadys Pharmaceuticals' HCV NS5B polymerase inhibitor research project.[17−20] To generate the model, the parameters of the conformational generation application (OMEGA[21]) and the docking engine (FRED[21]) were simultaneously optimized. We show that the optimization of the scoring function leads to a strong correlation coefficient (R^2) between the experimental activity and the optimized scoring function. The combination of the simultaneous optimization of the parameters, and the adjustment of the scoring function, resulted in R^2's of more than 0.66. While no crystal structures were solved for the inhibitors in this paper, we did compare the predicted binding modes using the Warfarin and the Flurbiprofen crystal structures and found good agreement, demonstrating the usefulness of the Autocorrelator.

2. METHODS

Autocorrelator Overview. The Autocorrelator is a software program that repeatedly executes a sequence of external programs while varying their input parameters in order to evaluate the dependency of the output on each parameter. The following example will focus on the use of the application with a docking protocol consisting of input preparation, conformer generation, docking, and scoring function fitting. The application uses a description of the sequence of programs to be executed in combination with the specification of the variable parameters and their value ranges to define the search space. The final step of any such protocol must be to compute a single floating-point value representing the quality of the results. In the following example, the correlation coefficient of the experimental log(IC_{50}) of a known set of ligands to the fitted docking scoring function is used as a quality criterion.

Three methods have been implemented as methods for the Autocorrelator to explore the parameter space:

- The *random method* performs a specified number of random trials varying the parameters.
- The *systematic method* explores all possible parameter values. Depending on the number of parameters and the number of allowed values for each parameter frequently renders this method unfeasible.
- The *evolutionary method* uses an evolutionary algorithm[22] to efficiently sample the configuration space and optimize the result quality.

In the docking example each method executes the whole docking protocol multiple times on a set of training molecules while varying parameters for each application in the protocol. The random and systematic methods simply report the quality for each evaluated set of parameters. The random method is helpful in finding acceptable starting values if no prior information is known. The systematic method allows the complete exploration of a limited configuration space. The evolutionary method is the method of choice for all but the simplest applications. It uses the result quality of past executions to vary the parameter for future executions as described below. As we believe it to be the most useful, the evolutionary method is discussed in further detail in the following paragraphs.

The evolutionary method initially computes a small number of models by choosing random settings within the parameter space for each model. Each set of parameters becomes a member of the parent population for the first cycle of the evolutionary algorithm. In each cycle, a child population is created by applying crossover and mutation operations to members of the parent population. A crossover of two sets of parameters is accomplished by selecting a random crossover point cp and using the first cp parameter values from the first parameter set and the remaining parameter values from the second set. Mutations are accomplished by randomly changing parameter values within the configured limits. Parent population size, child population size, and mutation rate are user adjustable properties. In initial experiments we found that a parent population size of 30, a child population size of 20, and a mutation rate of 20% gave good results. To optimize the utilization of our computational cluster we allow a new cycle to start as soon as 80% of the protocols from the previous cycle are completed. The results of the remaining protocols are considered in subsequent runs.

Our initial approach was to use the correlation coefficient R^2 between the model scores and the experimental results as fitness directly. However, this yielded models with high numbers of training set compounds that were unable to be docked in the computational process. Therefore the following fitness function was used:

$$\text{fitness} = R^2\left(\frac{n_s}{n_t}\right)^2 \quad (1)$$

In eq 1, n_s is the number of training compounds that are able to be docked in the protocol execution; n_t is the total number of compounds to be processed. Using eq 1, the protocols that are unable to account for all of the molecules in the training set are penalized.

The Autocorrelator was developed in Java, and the source code is freely available. It uses the OpenEye OEChem Toolkit[21] for parsing and transforming the input files, the statistical package R[23] for fitting the scoring function and the Sun Grid Engine[24] to execute the docking protocols on a distributed

computing cluster.[25] The specific application described below additionally used OMEGA[26] to generate small molecule conformers and FRED to dock the conformers into a protein and to compute the scoring function components.

Autocorrelator Job Setup. The Autocorrelator configuration file shown in Figure 1 is used to setup an

```
 1:<autoCorrelator>
 2:   <load id='molSource' type='molecules'>
 3:      <parameters>
 4:         <parameter name='sql'>
 5:            <value>select smi, id, log(10,ic50) from database_table</value>
 6:         </parameter>
 7:      </parameters>
 8:   </load>
 9:   <job id='o2' type='omega2' numberOfExecutions='15'>
10:      <parameters>
11:         <parameter name='maxconfs' numType='int' type='range'
12:                    from='60' to='300' step='20'/>
13:         <parameter name='ewindow' numType='int' type='range'
14:                    from='10' to='36'  step='5'/>
15-25:      ●●●
26:      </parameters>
27:      <job id='f1' type='fred2.1' numberOfExecutions='15'>
28:         <parameters>
29:            <parameter name='neg_img_size' type='list'>
30:               <value>small</value>
31:               <value>normal</value>
32:               <value>large</value>
33:               <value>xlarge</value>
34:            </parameter>
35:            <parameter name='scoring' type='list'>
36:               <value>plp</value>
37:               <value>shapegauss</value>
38:               <value>chemgauss2</value>
39:               <value>chemscore</value>
40:               <value>screenscore</value>
41:               <value>zapbind</value>
42:            </parameter>
43:            <parameter name='clash_scale' type='range'
44:                       from='0.4' to='1' step='.1'/>
45:            <parameter name='addbox' type='range'
46:                       from='1' to='10' step='.5'/>
47-57:         ●●●
58:         </parameters>
59:         <job id='r' type='R'>
60:           <parameters>
61:            <parameter name='numberOfVariables' type='list'>
62:               <value>3</value>
63:            </parameter>
64:            <parameter name='method' type='list'>
65:               <value>lars</value>
66:            </parameter>
67:            </parameters>
68:         </job><!--R-->
69:      </job>   <!--Fred-->
70:   </job>      <!--omega-->
71:</autoCorrelator>
```

Figure 1. Example of an Autocorrelator XML file. This file specifies what applications should run, in what order, and which parameters should be varied. Some parameters have been omitted (indicated by ●●●) to increase readability.

Autocorrelator run for a docking protocol. The configuration file describes a protocol as a load task followed by a sequence of jobs. The load task (lines 2−8) provides the input data. In the example presented in this paper, this is done by querying the ARISE[27] database via a SQL SELECT statement that retrieves structures and IC_{50} values. The sequence of jobs in the example file consists of the conformer generation job using OMEGA (lines 9−26), followed by the docking job (lines 27−58) using FRED and the evaluation job using R (lines 59−68) to fit the scoring function. The configuration file also specifies which parameters are to be explored for each job within the protocol. For OMEGA, the maxconfs (line 11) and ewindow (line 13) parameters are explored. For FRED the neg_img_size, scoring, clash_scale, and addbox parameters are explored (lines 29, 35, 43, and 45, respectively). Numerical parameters are divided into a fixed number of discrete values (e.g., line 11). The final task must return a quality value. In the example presented here, the LARS method[28] within the R[23] statistical software package is used. The LARS method is used to perform variable selection, creating a linear model with up to three terms of the scoring function. The correlation coefficient of the fitted scoring function to the experimental IC_{50} values retrieved in the load task is returned as quality of a given protocol execution.

Protein Structure Preparation. Two CYP2C9 structures bound to flurbiprofen (PDB code: 1R9O)[11] and warfarin (PDB code: 1OG5)[10] were used for computational modeling. All bound ions and water molecules were removed using PyMol.[29] Hydrogen atoms were added using Reduce.[30]

IC_{50} Determination. The Invitrogen Vivid CYP450 screening kit was used to measure CYP2C9 IC_{50} values for the NS5B inhibitors. The enzyme mix (CYP450 BACULOSOMES containing human CYP2C9 and rabbit NADPH-P450 reductase and the regeneration system) plus the test compounds were mixed together and preincubated for 20 min at room temperature. The reactions were then initiated by the addition of the Vivid BOMF substrate and the cofactor $NADP^+$. The strength of the inhibitors was determined by measuring the fluorescence of the BOMF metabolite product over time using the excitation and emission values of 485 and 530 nm, respectively. The data were collected on a SpectraMax M2 (Molecular Devices). The IC_{50} values were calculated from the dose-dependence of inhibition of product formation during the steady state reaction by fitting to a standard 4-parameter logistic equation.

CYP2C9 Training Set. Two related novel series of HCV NS5B polymerase inhibitors containing benzothiadiazine[17,18,20] and dioxoisothiazole[19] cores were identified at Anadys Pharmaceuticals (Figure 2). Members of these series were

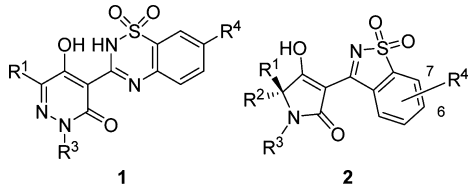

Figure 2. Core structures of the benzothiadiazine (**1**) and dioxoisothiazole (**2**) series of NS5B inhibitors.

found to be inhibitors of CYP2C9. To better understand the structure activity relationship (SAR) around the benzothiadiazine and dioxoisothiazole cores, the Autocorrelator was employed to generate models, using experimentally determined $\log(IC_{50})$ values for 58 molecules as the training set. The potencies of compounds in the training set against CYP2C9 range from double-digit nanomolar to micromolar. The training set did not possess any inactive molecules for CYP2C9 as, at the time of creation of the training set, every molecule within the benzothiadiazine and dioxoisothiazole chemotypes were active against CYP2C9.

Autocorrelator Parameters. The Autocorrelator used the conformational enumeration application OMEGA and docking application FRED in model generation. Correlation coefficients were calculated using the LARS methodology, selecting three components of the FRED scoring function. The genetic algorithm search strategy was chosen for our Autocorrelator investigation, with the defaults described above (a parent population size of 30, a child population size of 20, a mutation rate of 20%, and a maximum of 350 cycles).

The parameters that were chosen to be varied are known to have a significant impact on the quality of docking runs (Figure 1). For OMEGA, the parameters chosen were the maxconfs (maximum conformations) and ewindow (the energy window for allowable conformations) as well as a custom torsion library. Crystal structures of the benzothiadiazine compounds have consistently shown a planar conformation. To ensure that these

dx.doi.org/10.1021/ci200558e | J. Chem. Inf. Model. 2012, 52, 1328−1336

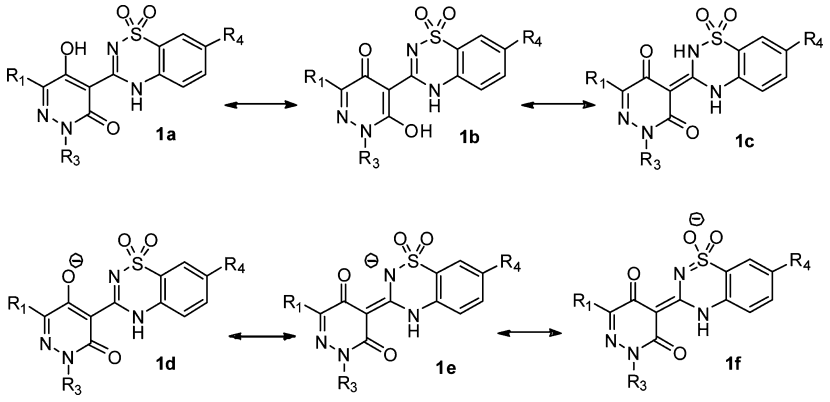

Figure 3. Tautomers of the benzothiadiazine (core **1**) HCV NS5B inhibitors (**1a**−**1c**) and resonance structures (**1d**−**1f**) of the deprotonated benzothiadiazine anions.

conformations were sampled, a custom torsion library file was created to enforce a 0 or 180 degree torsion angle around the biphenyl bond for both chemotypes, to replicate the dihedral seen in these molecules in crystal structures of NS5B polymerase (PDB accession codes: 3GYN, 3H2L, 3IGV, 3E51, 3D28, 3D5M, 3CVK, 3CWJ, 3CDE, 3CO9, 3BR9, 3BSA, and 3BSC).[31] For FRED, the parameters selected were the tstep (translational step size), rstep (rotational step size), neg_img_size (defining the size of the negative image), clash_scale (setting the tolerance for van der Waals interactions), addbox (defining the allowable search space around the cocrystallized ligand), optimization (for refinement), refine (whether or not a MMFF minimization is performed postdocking), exhaustive_scoring (more scoring), and scoring (the scoring function selected). In addition, we also elected to use SMIRKS based transformations of cores **1** and **2**. Examples of these transformations are shown in Figure 3. These transformations convert the input structures into a consistent charge and tautomeric forms.

3. RESULTS

Using the evolutionary algorithm of the Autocorrelator, models were created in 6 days on ∼165 nodes of our heterogeneous compute cluster. The performance characteristics of the cluster nodes ranged from 1 GHz Pentium 3 processors to 3.4 GHz Xeon processors. In the discussion below, the model derived from the warfarin cocrystal structure (PDB code: 1OG5) is referred to as *model A* and that from the flurbiprofen cocrystal structure (PDB code: 1RO9) is referred to as *model B*. The evolution of the fitness of the best models (A and B) over the course of the optimization is given in Figure 4. Optimizations were terminated after 350 cycles. In both structures, models of reasonable quality ($R^2 > 0.50$) were created within the first 100 cycles. Convergence for model B occurs in less than 300 cycles with a correlation coefficient of 0.66. Models constructed during the evolution of model A were stronger throughout model construction and converged after just 300 steps. Model A produced a stronger correlation coefficient of 0.73 than model B. Since evolutionary algorithms rely on random selection, the Autocorrelator was run multiple times for both systems. Repeated runs using the same parameters yielded models with fitness values between 0.62 and 0.73.

The parameters of the best model chosen by the Autocorrelator are shown in Table 1, as well as the number of possible choices that the Autocorrelator had for each parameter. The size of the search space (the number of possible

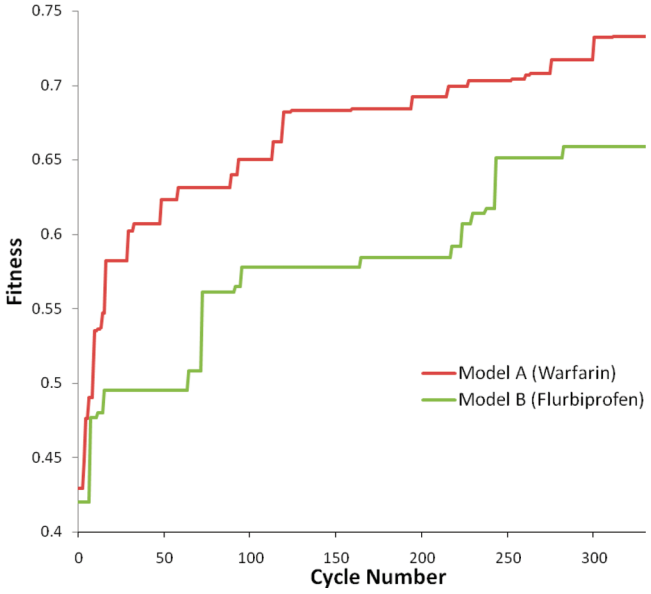

Figure 4. Fitness of the best model found for each cycle of the Autocorrelator during the optimization of models A and B. The fitness of each cycle is the correlation coefficient of the LARS derived scoring function with the penalty for models that were unsuccessful at docking all inhibitors as shown in eq 1.

models) is simply a combination of the available choices, which for the given parameters is 3 764 517 120 possible models.

Model A (Warfarin Model). In model A, we found that the best conformational enumeration conditions used the modified torsion library, a 10 kcal energy window, and a maximum of 220 conformations. The best docking conditions were using the Screenscore scoring function with a PLP (pairwise linear potential) optimization, a MMFF (Merck molecular force field) refinement and a 10 Å box (beyond the smallest box that would contain warfarin). The Autocorrelator selected a deprotonated species of our molecules (Table 1). A strong correlation between the rebalanced scoring function and the experimental IC_{50} values is seen (Figure 5). All molecules in the training set were able to be docked and all data points reside within one log of the trend line (rms error 0.33).

The Autocorrelator run evaluated a total of 7225 models. By analyzing average fitness values for each parameter individually, we are able to estimate the sensitivity of the results from each parameter and to deduce preferred ranges for each parameter.

dx.doi.org/10.1021/ci200558e | J. Chem. Inf. Model. 2012, 52, 1328−1336

Table 1. Parameter Varied during the Evolutionary Optimization of CYP2C9 Models and Final Optimized Parameter Values

parameter	range	possible values	final value model A[a]	final value model B[b]
ligand valence structure	cf. Figure 3	6	**1f**	**1d**
OMEGA				
Maxconfs	60−300	13	220	220
Ewindow	10−35	6	10	15
torsion library		2	custom	default
FRED				
scoring		6	screenscore	screenscore
optimization		6	Plp	chemgauss2
exhaustive_scoring		3	shapegauss	chemgauss2
neg_img_size		4	na[c]	na[c]
refine		2	lig_mmff	no_refinement
Clash_scale	0.4−1.0	7	0.8	0.6
Addbox	1−10	19	10.0	6.0
rStep	0.8−2.0	7	1.4	1.4
tStep	0.6−1.4	5	1.0	1.0

[a]Best model built using the warfarin cocrystal structure. [b]Best model built using the flurbiprofen cocrystal structure. [c]This parameter did not change the computational results.

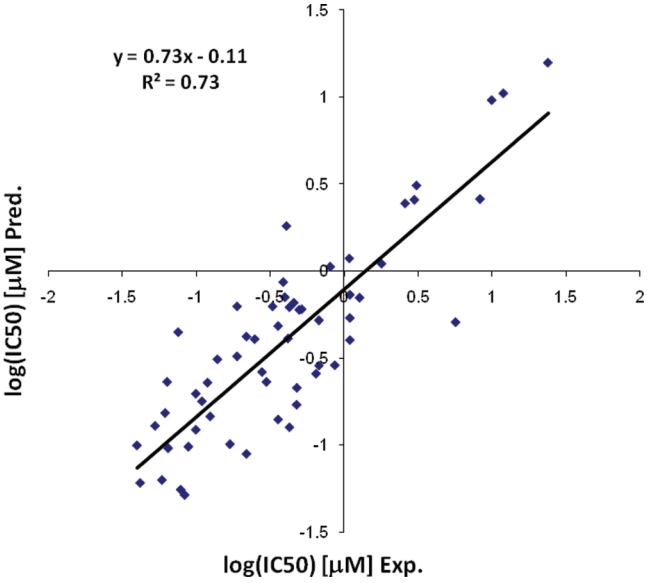

Figure 5. Correlation of predicted and experimentally determined IC_{50} values for the best model generated in model A. All 58 molecules in the training set were docked.

For conformation generation, the maxconf parameter should be set to 100 or higher, while the optimal range for the ewindow parameter is between 5 and 10 kcal/mol. For FRED, the optimal range for the clashscore was between 0.64 and 0.72; for addbox, a value higher than 10 was optimal. The optimal ranges for step sizes for rotational and translational transformations were less well-defined with optimal values around 1.4 for rstep and 1.0 for tstep.

Strong correlations are dependent on the addbox parameter in model A. Shrinking the addbox parameter from 10 to 9 Å reduced the correlation from 0.733 to 0.654. Further reduction of the box size to 8 Å lowers the correlation to 0.24. Tautomer selection was another variable that greatly impacted the results of our runs. A marked difference in the correlation coefficient was seen between tautomer **1f** of 0.73 and all of the other tautomers, which produced models with scores ranging from 0.487 to 0.376.

The Autocorrelator found that the $\log(IC_{50})$ values of the training set are best described by the formula below (eq 2):

$$\log(IC_{50}) = (\text{Screenscore.LIPO}[-0.0526]) + (\text{Screenscore.HB}[-0.169]) + (\text{Screenscore.AMBIG}[0.0478]) - 0.395 \quad (2)$$

The optimized scoring function for model A is given in eq 2. This equation was generated by the LARS (least-angle regression) algorithm implemented in R. LARS selects which components from the scoring function should be included in the linear regression and then calculates the appropriate coefficients for each term. These coefficients dervived from LARS show that inhibitors, scored with more negative values in the lipophilic and hydrogen-bonding terms, are predicted to be more potent inhibitors of CYP2C9. This is understandable as molecules with stronger *van der Waals* and hydrogen-bonding interactions would be expected to be more potent against a target.

We see consensus in the docking solutions returned by FRED in model A. A supermajority (92%) of the docking poses orient the ligands similar to Figure 6. These docking solutions leave the $R_{1\&2}$ and R_3 groups close to the heme. The R_4 group is oriented away from the heme irrespective of the functional group. We only have the two different R_4 groups (the acetamide and the sulfonamide) in the training set, and they adopt two different patterns of hydrogen-bonding interactions with Asn107 and Arg108. All docking poses locate the ligands at least 6 Å away from the crystallographic position of warfarin.

Model B (the Flurbiprofen Model). In model B, we found that the best conformational enumeration conditions used a 15 kcal energy window, the default torsion library and a maximum of 220 conformations. The best docking conditions use the Screenscore scoring function with a chemgauss2 optimization, no MMFF refinement, and a 6 Å box (beyond the smallest box around flurbiprofen). The correlations between the computational and experimentally determined IC_{50} values are shown in Figure 7. A majority of the points reside within one log of the trendline, and all molecules in the training set were able to be docked (rms error 0.38).

dx.doi.org/10.1021/ci200558e | J. Chem. Inf. Model. 2012, 52, 1328−1336

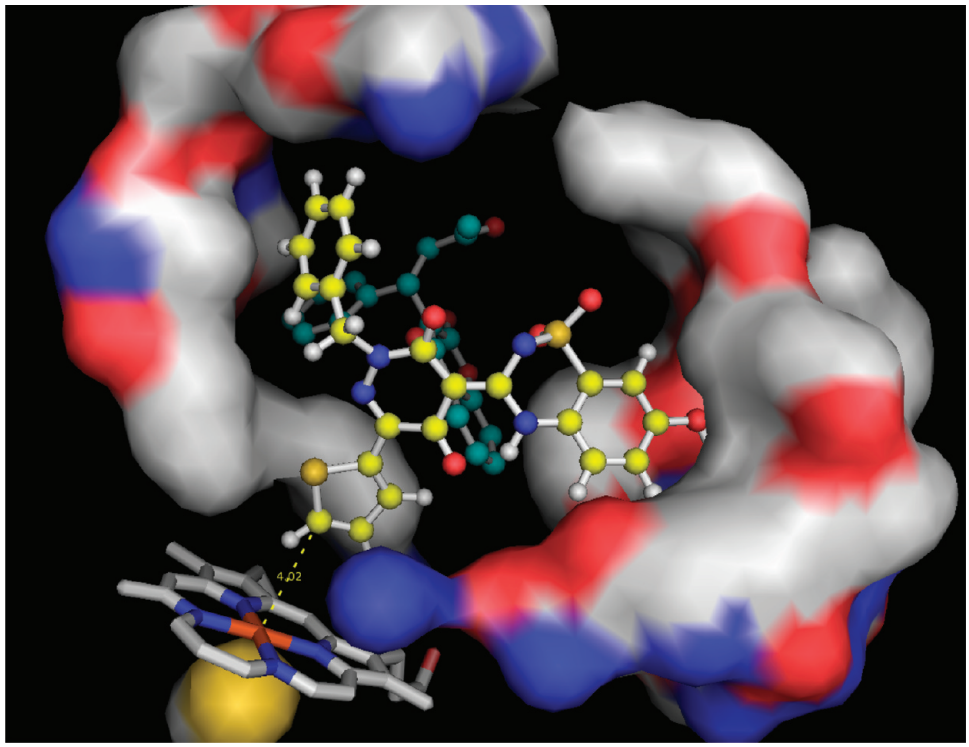

Figure 6. Docking solution for one compound as predicted by model A in the warfarin cocrystal structure. The thiophene (R_1) is in close proximity of the catalytic heme (4 Å). The ligand (yellow) docked with our optimum conditions reside far removed from the location of warfarin (blue).

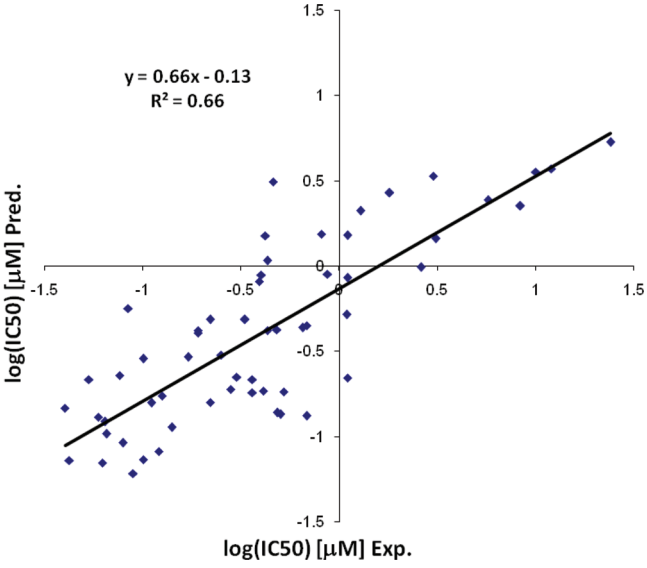

Figure 7. Correlation of predicted and experimentally determined IC_{50} values for the best model generated in model B. Fifty-eight compounds were used as a training set and are docked in this model.

The Autocorrelator found that the log(IC_{50}) values of the training set are best described by the formula below (eq 3):

$$\log(IC_{50}) = (0.0132\text{Screenscore}) + (\text{Screenscore.HB}[-0.303]) + (\text{Screenscore.ARO}[-0.255]) + 6.483 \quad (3)$$

In model B, the Autocorrelator has selected the same scoring function to describe the training set of molecules as it did in model A. The components of the scoring function were selected by LARS, as they were in model A. As before, LARS chose similar terms as it did in model A. As shown in eqs 2 and 3, the hydrogen bonding and lipophillic scoring terms were found to correlate strongly with the log(IC_{50}). This time the Autocorrelator chose the aromatic scoring term over the lipo scoring term. Again the terms that constitute eq 3 are in agreement with expectations. Molecules that have better hydrogen bonding or stronger aromatic interactions are predicted to be more potent.

4. DISCUSSION

The Autocorrelator has been used to generate models describing the CYP2C9 activity of a set of HCV NS5B polymerase inhibitors. Two different structures of CYP2C9 were used and the Autocorrelator was able to generate strong models with both of them. Models A and B have produced results that orient the training molecules in a similar orientation within two different conformations of CYP2C9 (Figures 6 and 8). These solutions both select resonance structures that are negatively charged. This is consistent with other findings that report that there is a known negative charge preference of CYP2C9.[32] In both models (eq 2 and 3) similar scoring function terms were selected in the rebalanced scoring functions. These terms indicate that stronger hydrogen-bonding interactions, better packing of the hydrophobic surface, and better aromatic interactions lead to tighter binders of CYP2C9. The Autocorrelator even selected the same scoring function for both systems.

The necessity of a larger box size to construct strongly correlating models was unexpected. The ligands, in both crystal structures, are smaller than our inhibitors. Thus a small increase in the box size was expected to accommodate our larger inhibitors. What was unexpected was the magnitude required. In model A, we had expected solutions that would have our

dx.doi.org/10.1021/ci200558e | J. Chem. Inf. Model. 2012, 52, 1328−1336

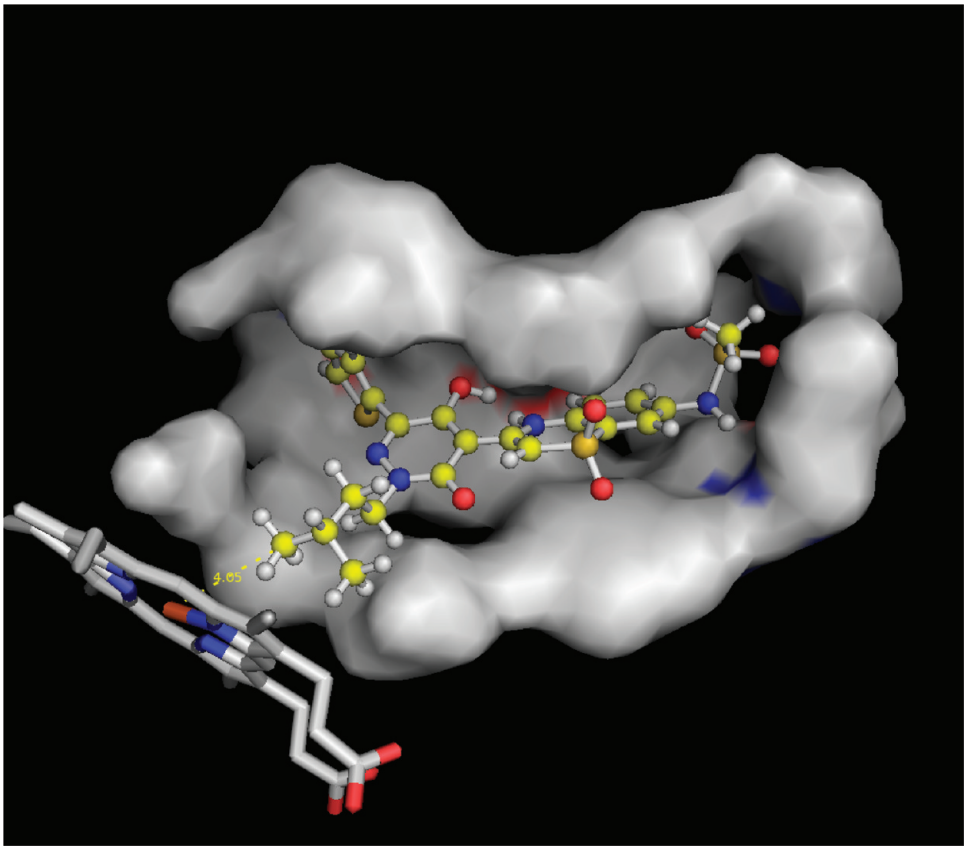

Figure 8. Inhibitor docked in close proximity to the heme in the flurbiprofen cocrystal structure (PDB code: 1RO9). The isopentane side chain (R_2) is 4.05 Å away from the heme.

molecules docked in close proximity to the location of warfarin (which is 10 Å away from the heme). Instead, the larger boxsize leads to the molecules docked in closer proximity to the reactive center of CYP2C9 and in general alignment with poses seen in model B.

In models A and B the inhibitors are docked with the core of the ligands and R_4 oriented in the same direction. Variance can be seen in the orientation of the $R_{1\&2}$ and R_3 groups, either of which can point toward the heme. We hypothesize that these molecules transition between the protonated and deprotonated states, allowing the left-hand side (functional group) of the molecule to rotate. This allows the ligand to select the sterically better tolerated substituent (either $R_{1\&2}$ or R_3) to be placed near the heme. The rotation of the $R_{1\&2}$ and R_3 groups has been seen previously in cocrystal structures of these molecules with NS5B (PDB codes: 3GYN, 3H2L, 3IGV, 3E51, 3D28, 3D5M, 3CVK, 3CWJ, 3CDE, 3CO9, 3BR9, 3BSA, and 3BSC).[31]

While only one example is presented in this paper, we believe that in the present industrial environment, where computational chemists are expected to be able to do more in less time, the Autocorrelator provides many unique advantages. Thousands of computational experiments can be evaluated without human intervention and the models generated are often of high quality. The Autocorrelator can drive numerous applications. As presently implemented, it can execute ROCS, EON, SZYBKI, and GOLD in addition to OMEGA and FRED shown here. The Autocorrelator is capable of evaluating and optimizing the results of any application that can be driven from the command line, and once encapsulated an application can be easily integrated into any functional pipeline.

All Autocorrelator runs start from 2D ligand structures, and the results of these runs can be used as a recipe. These instructions are useful for noncomputational chemists as they can be easily integrated into a web platform. We have used these recipes ourselves in our platform the Illuminator platform and have seen firsthand the efficiency gains possible when high quality computational models are deployed sitewide.[3]

5. CONCLUSION

We have developed an automated model builder, the Autocorrelator, and have used this new tool to construct a model that predicts the CYP2C9 activity within our chemotypes. While the autonomously derived CYP2C9 models described in this paper correlate strongly with experimental results, we believe that the evaluation of Autocorrelator models requires human intervention to validate that the computationally derived models are of sufficient quality and robustness. The Autocorrelator-generated CYP2C9 models for the two systems shown here are quite similar. Our models position the compounds in a similar orientation, use the same scoring function and similar terms to describe potency, and require the same charge state. This overlap between these models increases our confidence in their use and thus the effectiveness of the Autocorrelator. The application of these models to new compounds will however be the ultimate validation of the models. In our experience, the Autocorrelator greatly increases the productivity of computational chemists while improving model quality.

AUTHOR INFORMATION

Corresponding Author

*E-mail: matthew.lardy@takedasd.com.

Present Addresses

[†]Takeda San Diego, 10410 Science Center Drive, San Diego, CA 92121.

[‡]CelGene Signal Research, 4550 Towne Centre Court, San Diego, CA 92121.

[§]Molecular Kinetics, Inc., 6201 La Pas Trail, Suite 160, Indianapolis, IN 46268.

[⊥]Genentech Inc., 1 DNA Way, South San Franscisco, CA 94080.

Notes

The authors declare no competing financial interest.

ACKNOWLEDGMENTS

We would like to thank the Anadys management, Drs. S. Worland, J. Appleman, D. Averett, and S. Webber for supporting the implementation of the Anadys Computational Platform.

REFERENCES

(1) Ertl, P.; Selzer, P.; Mühlbacher, J. Web-based cheminformatics tools deployed via corporate Intranets. *Drug Discovery Today: BIOSILICO* **2004**, *2*, 201−207.

(2) Stewart, K. D.; Shiroda, M.; James, C. A. Drug Guru: A computer software program for drug design using medicinal chemistry rules. *Bioorg. Med. Chem.* **2006**, *14*, 7011−7022.

(3) Gobbi, A.; Lardy, M.; Kim, S. H.; Ruebsam, F.; Tran, M.; Webber, S. E.; Xiang, A. Illuminator: Increasing synergies between medicinal and computational chemists. *Cheminformatics* **2010**, *3*, 1−9.

(4) Danielson, P. B. The cytochrome P450 superfamily: biochemistry, evolution and drug metabolism in humans. *Curr. Drug Metab.* **2002**, *3*, 561−597.

(5) Hodgson, J. ADMET—turning chemicals into drugs. *Nat. Biotechnol.* **2001**, *19*, 722−726.

(6) Shardlow, C. E.; Generaux, G. T.; MacLauchlin, C. C.; Pons, N.; Skordos, K. W.; Bloomer, J. C. Utilising Drug-drug Interaction Prediction Tools During Drug Development: Enhanced Decision-making Based on Clinical Risk. *Drug Metab. Dispos.* **2011**, *39*, 2076−2084.

(7) Byvatov, E.; Baringhaus, K.; Schneider, G.; Matter, H. A Virtual Screening Filter for Identification of Cytochrome P450 2C9 (CYP2C9) Inhibitors. *QSAR Comb. Sci.* **2007**, *26* (5), 618−628.

(8) Polgár, T.; Menyhárd, D.; Keserű, G. Effective virtual screening protocol for CYP2C9 ligands using a screening site constructed from flurbiprofen and S-warfarin pockets. *J. Comput.-Aided Mol. Des.* **2007**, *21*, 539−548.

(9) Ekins, S.; De Groot, M. J.; Jones, J. P. Pharmacophore and Three Dimensional Quantitative Structure Relationship Methods for Modeling Cytochrome P450 Active Sites. *Drug Metab. Dispos.* **2001**, *29* (7), 936−945.

(10) Williams, P. A.; Cosme, J.; Ward, A.; Angove, H. C.; Matak Vinkovic, D.; Jhoti, H. Crystal structure of human cytochrome P450 2C9 with bound warfarin. *Nature* **2003**, *424*, 464−468.

(11) Wester, M. R.; Yano, J. K.; Schoch, G. A.; Yang, C.; Griffin, K. J.; Stout, C. D.; Johnson, E. F. The structure of human cytochrome P450 2C9 complexed with flurbiprofen at 2.0-A resolution. *J. Biol. Chem.* **2004**, *279*, 35630−35637.

(12) Afzelus, L.; Zamora, I.; Ridderström, M.; Andersson, T. B.; Karlén, A.; Collen, M.; Masimirembwa, C. M. Competitive CYP2C9 Inhibitors: Enzyme Inhibition Studies, Protein Homology Modeling, and Three-Dimensional Quantitative Structure-Activity Relationship Analysis. *Mol. Pharmacol.* **2001**, *59* (4), 909−919.

(13) Andersson, C. D.; Thysell, E.; Lindström, A.; Bylesjö, M.; Raubacher, F.; Linusson, A. A Multivariate Approach to Investigate Docking Parameters' Effects on Docking Performance. *J. Chem. Inf. Model.* **2007**, *47*, 1673−1687.

(14) Jones, G.; Willett, P.; Glen, R. C. Molecular recognition of receptor sites using a genetic algorithm with a description of desolvation. *J. Mol. Biol.* **1995**, *245*, 43−53.

(15) McGann, M. R.; Almond, H. R.; Nicholls, A.; Grant, J. A.; Brown, F. K. Gaussian docking functions. *Biopolymers* **2003**, *68*, 76−90.

(16) The Autocorrelator is available at http://code.google.com/p/autocorrelator

(17) Ellis, D. A.; Blazel, J. K.; Tran, C. V.; Ruebsam, F; Murphy, D. E.; Li, L.; Zhao, J.; Zhou, Y.; McGuire, H. M.; Xiang, A. X.; Webber, S. E.; Zhao, Q.; Han, Q.; Kissinger, C. R.; Lardy, M.; Gobbi, A.; Showalter, R. E.; Shah, A. M.; Tsan, M.; Patel, R. A.; LeBrun, L. A.; Kamran, R.; Bartkowski, D. M.; Nolan, T. G.; Norris, D. A.; Sergeeva, M.; Kirkovsky, L. 5,5′-and 6,6′- Dialkyl-5,6-dihydro-1H-pyridin-2-ones as potent inhibitors of HCV NS5B polymerase. *Bioorg. Med. Chem. Lett.* **2009**, *19*, 6047−6052.

(18) Ellis, D. A.; Blazel, J. K.; Webber, S. E.; Tran, C. V.; Dragovich, P. S.; Sun, Z.; Ruebsam, F.; McGuire, H. M.; Xiang, A. X.; Zhao, J.; Li, L.-S.; Zhou, Y.; Han, Q.; Kissinger, C. R.; Showalter, R. E.; Lardy, M.; Shah, A. M.; Tsan, M.; Patel, R.; LeBrun, L. A.; Kamran, R.; Bartkowski, D. M.; Nolan, T. G.; Norris, D. A.; Sergeeva, M. V.; Kirkovsky, L. 4-(1,1-Dioxo-1,4-dihydro-1′-6-benzo[1,4]thiazin-3-yl)-5-hydroxy-2H-pyridazin-3-ones as potent inhibitors of HCV NS5B polymerase. *Bioorg. Med. Chem. Lett.* **2008**, *18*, 4628−4632.

(19) Kim, S. H.; Tran, M. T.; Ruebsam, F.; Xiang, A. X.; Ayida, B.; McGuire, H.; Ellis, D.; Blazel, J.; Tran, C. V.; Murphy, D. E.; Webber, S. E.; Zhou, Y.; Shah, A. M.; Tsan, M.; Showalter, R. E.; Patel, R.; Gobbi, A.; LeBrun, L. A.; Bartkowski, D. M.; Nolan, T. G.; Norris, D. A.; Sergeeva, M. V.; Kirkovsky, L.; Zhao, Q.; Han, Q.; Kissinger, C. R. Structure-based design, synthesis, and biological evaluation of 1,1-dioxoisothiazole and benz[b]thiophene-1,1-dioxide derivatives as novel inhibitors of hepatitis C virus NS5B polymerase. *Bioorg. Med. Chem. Lett.* **2008**, *18*, 4181−4185.

(20) Sergeeva, M. V.; Zhou, Y.; Bartkowski, D. M.; Nolan, T. G.; Norris, D. A.; Okamoto, E.; Kirkovsky, L.; Kamran, R.; LeBrun, L. A.; Tsan, M.; Patel, R.; Shah, A. M.; Lardy, M.; Gobbi, A.; Li, L.-S.; Zhao, J.; Bertolini, T.; Stankovic, N.; Sun, Z.; Murphy, D. E.; Webber, S. E.; Dragovich, P. S. Novel HCV NS5B polymerase inhibitors derived from 4-(1′,1′-dioxo-1′,4′-dihydro-1′,6-benzo[1′,2′,4′]thiadiazin-3′-yl)-5-hydroxy-2H-pyridazin-3-ones: Part 4. Optimization of DMPK properties. *Bioorg. Med. Chem. Lett.* **2008**, *18*, 3421−3426.

(21) The OEChem Toolkit, OMEGA, ROCS, FRED, and SZYBKI are distributed by OpenEye Scientific Software, Santa Fe, NM: http://www.eyesopen.com (accessed Sep 2007).

(22) (a) Gillet, V. J. *In Evolutionary Algorithms in Molecular Design*; Clark, D. E., Ed.; Wiley-VCH: Weinheim, Germany, 2000; Chapter 4, pp 49−69. (b) Lameijer, E. W.; Baeck, Th.; Kok, J.; IJzerman, A. P. Evolutionary algorithms in drug design. *Nat. Comput.* **2005**, *4*, 177−243.

(23) *R: A Language and Environment for Statistical Computing*, version 2.0.1; R Development Core Team: Vienna, Austria, 2004.

(24) Grid Engine Project Home. http://gridengine.sunsource.net/ (accessed Sep 2007).

(25) Bullard, D.; Gobbi, A.; Lardy, M. A.; Perkins, C.; Little, Z.; Hydra, A Self Regenerating High Performance Computing Grid for Drug Discovery. *J. Chem. Inf. Model.* **2008**, *48*, 811−816.

(26) Boström, J.; Greenwood, J. R.; Gottfries, J. Assessing the performance of OMEGA with respect to retrieving bioactive conformations. *J. Mol. Graphics Modell* **2003**, *21*, 449−462.

(27) Gobbi, A.; Funeriu, S.; Ioannou, J.; Wang, J.; Lee, M.-L.; Palmer, C.; Bamford, B.; Hewitt, R. Process-Driven Information Management System at a Biotech Company: Concept and Implementation. *J. Chem. Inf. Comp. Sci.* **2004**, *44*, 964−975.

(28) Efron, B; Hastie, T; Johnstone, I; Tibshirani, R. Least angle regression. *Ann. Statist.* **2004**, *32*, 407−499.

(29) DeLano, W. L. *The PyMOL Molecular Graphics System*, version 0.99; DeLano Scientific: Palo Alto, CA, USA, 2006; http://www.pymol.org.
(30) Word, J. M.; Lovell, S. C.; Richardson, J. S.; Richardson, D. C. Asparagine and glutamine: using hydrogen atom contacts in the choice of sidechain amide orientation. *J. Mol. Biol.* **1999**, *285*, 1733−1745.
(31) Research Collaboratory for Structural Bioinformatics, Rutgers University, New Brunswick, NJ. http://www.rcsb.org.
(32) Locuson, C. W., II; Rock, D. A.; Jones, J. P. Quantitative Binding Models for CYP2C9 Based on Benzbromarone Analogues. *Biochemistry* **2004**, *43* (22), 6948−6958.